NLO corrections to squark-squark production and decay at the LHC

in collaboration with W. Hollik and J. M. Lindert
based on arXiv:1207.xxxx

MAX-PLANCK-GESELLSCHAFT

Davide Pagani

Max Planck Institut für Physik, München

ICHEP, 5-7-2012, Melbourne

SUSY PARTICLES AT THE LHC

Production

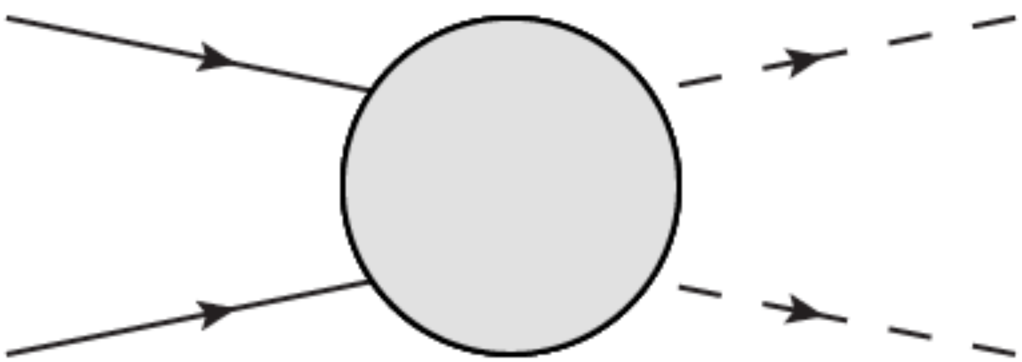

Decay

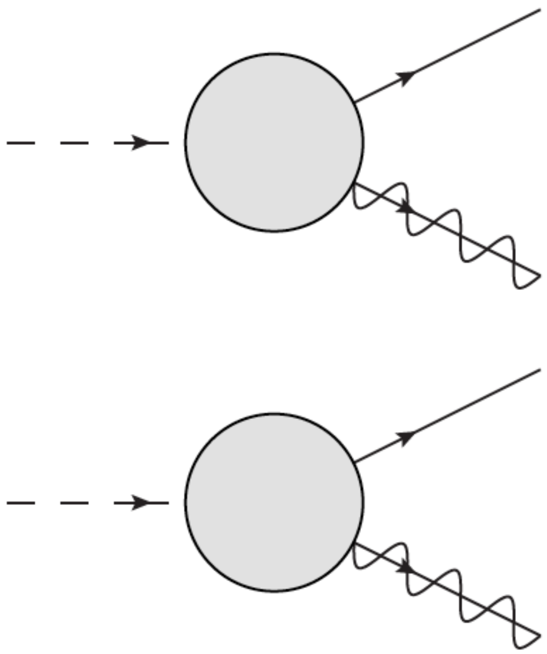

Squark-Squark:
NLO QCD: *Beenakker et al.'96*
NLO EW:*Germer et al. '10*
Beyond NLO (resummed):
Beneke, Falgari, Schwinn '10
Beenakker et al '09

Squark:
NLO QCD: *Djouadi, Hollik, Junger '96*
NLO EW:*Guasch, Hollik, Sola '02*

In order to study systematically the experimental signature emerging from SUSY particles, both corrections to production and decays must be included.

We study the experimental signature

$$2j + \not{E}_T(+X)$$

via squark-squark production and direct decay into the lightest neutralino

$$pp \to \tilde{q}\tilde{q}' \to qq'\tilde{\chi}_1^0\tilde{\chi}_1^0(+X)$$

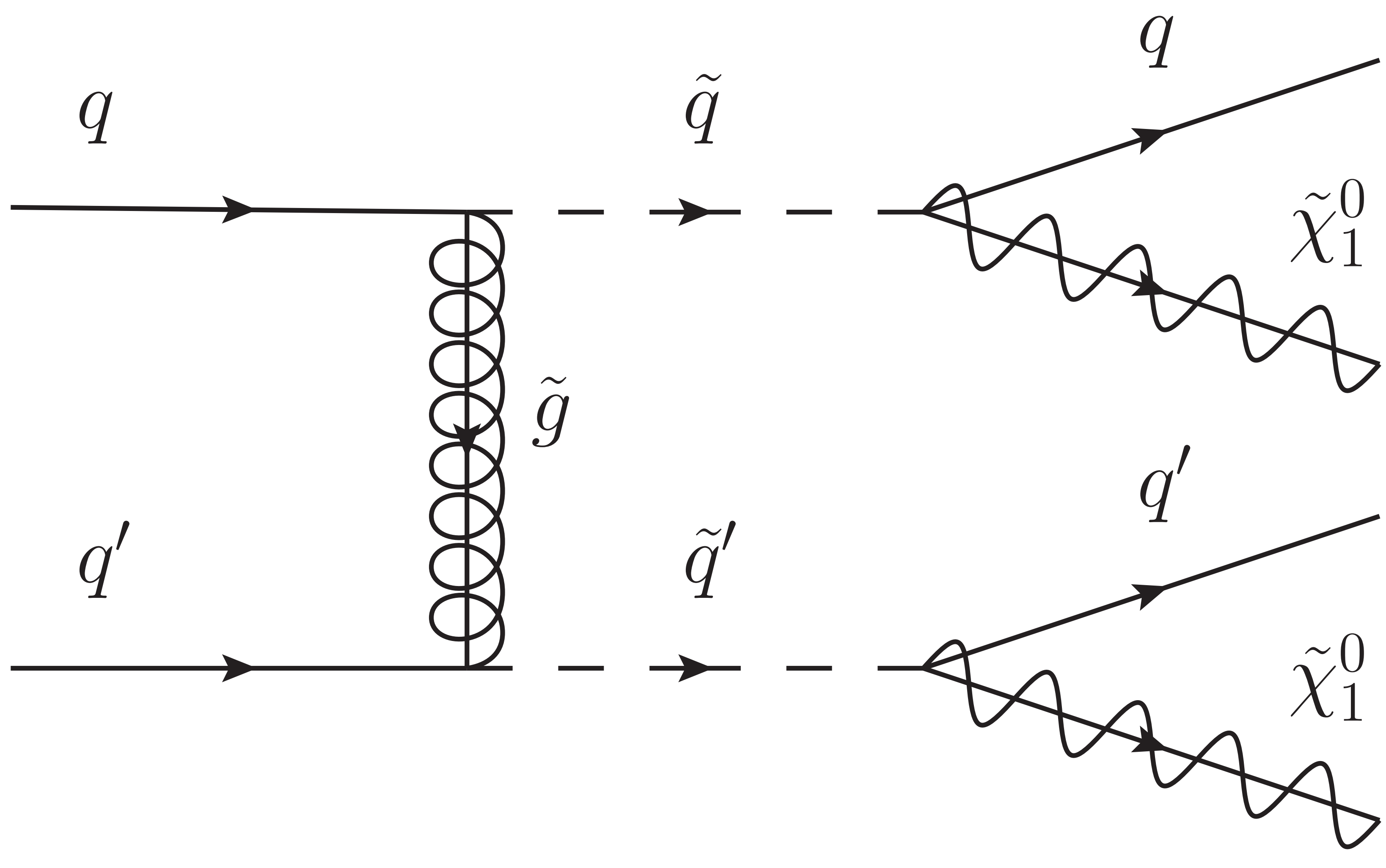

We study the experimental signature

$$2j + \not{E}_T (+X)$$

via squark-squark production and direct decay into the lightest neutralino

$$pp \to \tilde{q}\tilde{q}' \to qq'\tilde{\chi}_1^0\tilde{\chi}_1^0 (+X)$$

Standard procedure:

Producing events with a parton shower generator and rescaling the weights with the global K factor from NLO QCD corrections to the total cross-section of the squark-squark production.

We study the experimental signature

$$2j + \not{E}_T (+X)$$

via squark-squark production and direct decay into the lightest neutralino

$$pp \to \tilde{q}\tilde{q}' \to qq'\tilde{\chi}_1^0\tilde{\chi}_1^0(+X)$$

Standard procedure:

Producing events with a parton shower generator and rescaling the weights with the global K factor from NLO QCD corrections to the total cross-section of the squark-squark production

Our procedure:

Including fully differential NLO corrections to both the decay and production, where in the calculation all flavour and chirality configurations of intermediate squarks are treated independently.

BORN

$$qq' \to \tilde{q}\tilde{q}' \to q\tilde{\chi}_1^0 q'\tilde{\chi}_1^0$$

$$\Gamma_{\tilde{q}}/m_{\tilde{q}} \to 0 \qquad \boxed{\hat{\sigma}^{(0)}_{\mathrm{NWA}} = \hat{\sigma}^{(0)}(qq' \to \tilde{q}\tilde{q}') \times BR^{(0)}(\tilde{q} \to q\tilde{\chi}_1^0) \times BR^{(0)}(\tilde{q}' \to q'\tilde{\chi}_1^0)}$$

NLO in NWA

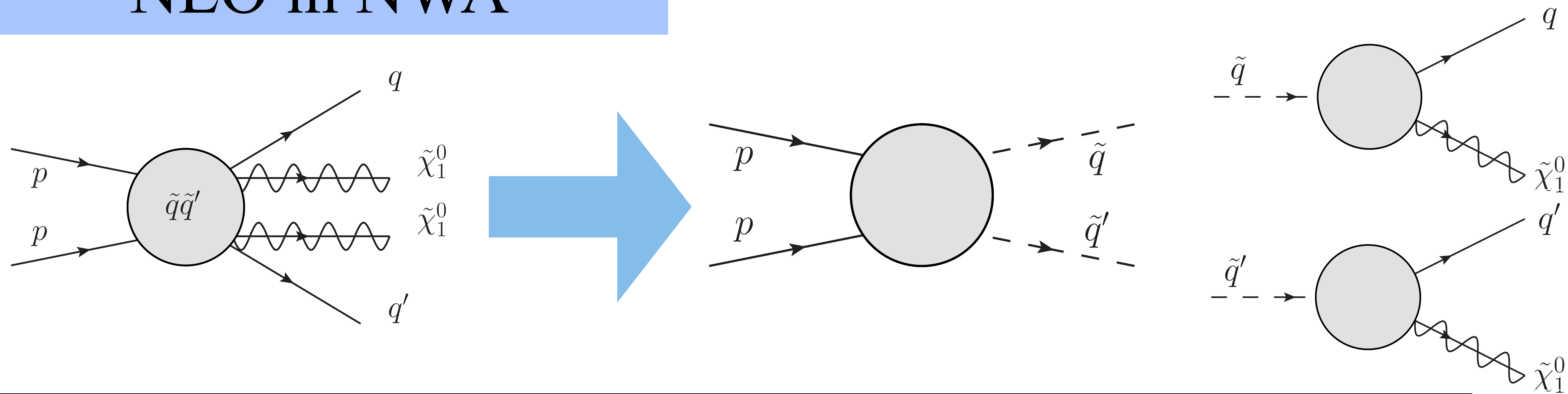

BORN

$$qq' \to \tilde{q}\tilde{q}' \to q\tilde{\chi}_1^0 q'\tilde{\chi}_1^0$$

$$\Gamma_{\tilde{q}}/m_{\tilde{q}} \to 0 \qquad \boxed{\hat{\sigma}^{(0)}_{\rm NWA} = \hat{\sigma}^{(0)}(qq' \to \tilde{q}\tilde{q}') \times BR^{(0)}(\tilde{q} \to q\tilde{\chi}_1^0) \times BR^{(0)}(\tilde{q}' \to q'\tilde{\chi}_1^0)}$$

NLO in NWA

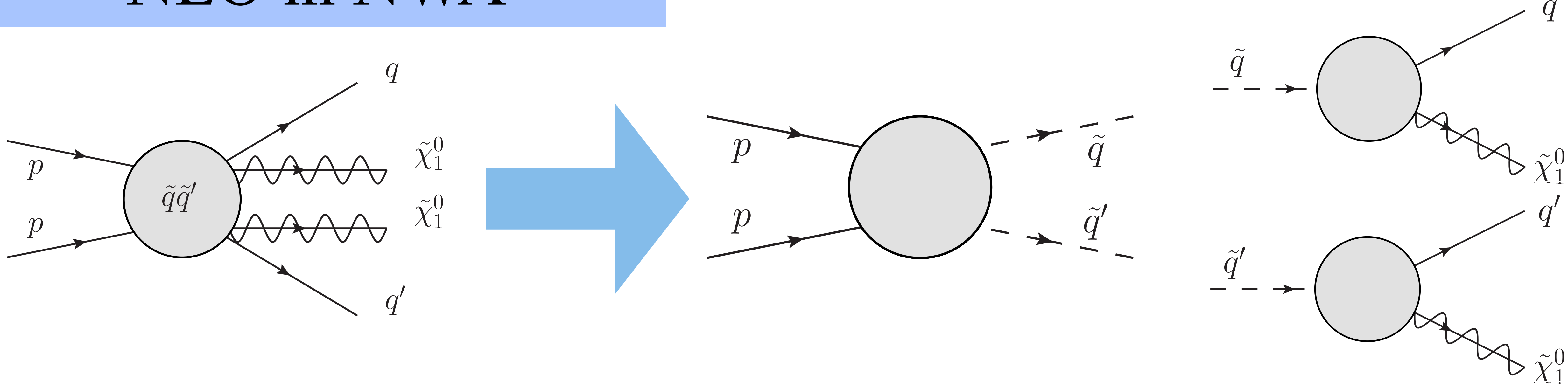

Formal expansion in α_s:

"master formula"

Born

$$d\sigma^{(0+1)}_{\rm NWA}(pp \to \tilde{q}\tilde{q}' \to q\tilde{\chi}_1^0 q'\tilde{\chi}_1^0(+X)) = \frac{1}{\Gamma^{(0)}_{\tilde{q}}\Gamma^{(0)}_{\tilde{q}'}}\Big[d\sigma^{(0)}_{pp\to\tilde{q}\tilde{q}'} d\Gamma^{(0)}_{\tilde{q}\to q\tilde{\chi}_1^0} d\Gamma^{(0)}_{\tilde{q}'\to q'\tilde{\chi}_1^0}\Big(1 - \frac{\Gamma^{(1)}_{\tilde{q}}}{\Gamma^{(0)}_{\tilde{q}}} - \frac{\Gamma^{(1)}_{\tilde{q}'}}{\Gamma^{(0)}_{\tilde{q}'}}\Big)$$

NLO decay

$$+d\sigma^{(0)}_{pp\to\tilde{q}\tilde{q}'} d\Gamma^{(1)}_{\tilde{q}\to q\tilde{\chi}_1^0} d\Gamma^{(0)}_{\tilde{q}'\to q'\tilde{\chi}_1^0} + d\sigma^{(0)}_{pp\to\tilde{q}\tilde{q}'} d\Gamma^{(0)}_{\tilde{q}\to q\tilde{\chi}_1^0} d\Gamma^{(1)}_{\tilde{q}'\to q'\tilde{\chi}_1^0}$$

NLO production

$$+d\sigma^{(1)}_{pp\to\tilde{q}\tilde{q}'} d\Gamma^{(0)}_{\tilde{q}\to q\tilde{\chi}_1^0} d\Gamma^{(0)}_{\tilde{q}'\to q'\tilde{\chi}_1^0}\Big]$$

NLO production

For every chirality and flavour configuration:

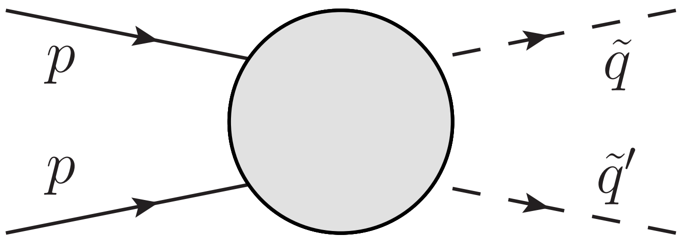

$$d\sigma^{(1)}_{pp\to\tilde{q}\tilde{q}'(+X)} = d\sigma^{\text{virtual+soft}}_{pp\to\tilde{q}\tilde{q}'(g)} + d\sigma^{\text{coll}}_{pp\to\tilde{q}\tilde{q}'(g)} + d\sigma^{\text{hard}}_{pp\to\tilde{q}\tilde{q}'g} + d\sigma^{\text{real-quark}}_{pp\to\tilde{q}\tilde{q}'\bar{q}^{(\prime)}}$$

Fully differential cross-section

NLO production

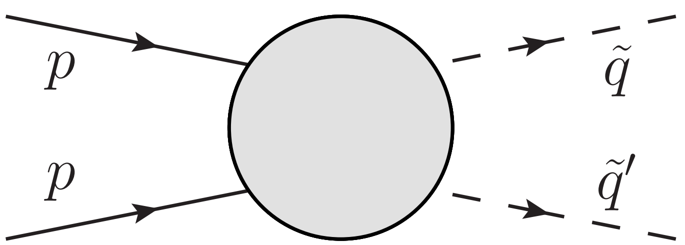

For every chirality and flavour configuration:

$$d\sigma^{(1)}_{pp\to\tilde{q}\tilde{q}'(+X)} = d\sigma^{\text{virtual+soft}}_{pp\to\tilde{q}\tilde{q}'(g)} + d\sigma^{\text{coll}}_{pp\to\tilde{q}\tilde{q}'(g)} + d\sigma^{\text{hard}}_{pp\to\tilde{q}\tilde{q}'g} + d\sigma^{\text{real-quark}}_{pp\to\tilde{q}\tilde{q}'\bar{q}^{(\prime)}}$$

Fully differential cross-section

NLO decay

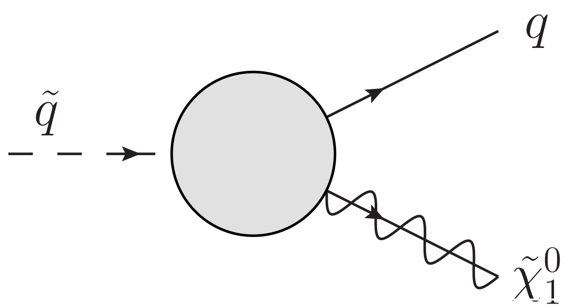

$$d\Gamma^{(1)}_{\tilde{q}\to q\tilde{\chi}^0_1} = d\Gamma^{\text{virtual+soft}}_{\tilde{q}\to q\tilde{\chi}^0_1(g)} + d\Gamma^{\text{coll}}_{\tilde{q}\to q\tilde{\chi}^0_1(g)} + d\Gamma^{\text{hard}}_{\tilde{q}\to q\tilde{\chi}^0_1 g}$$

Fully differential decay

NLO production

For every chirality and flavour configuration:

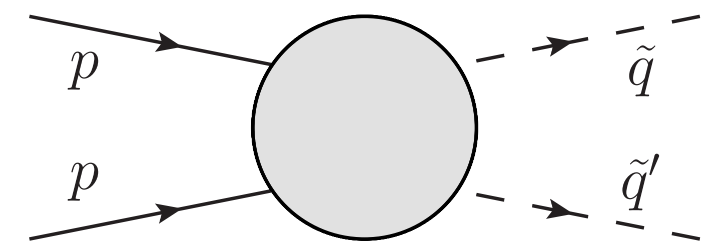

$$d\sigma^{(1)}_{pp\to\tilde{q}\tilde{q}'(+X)} = d\sigma^{\text{virtual+soft}}_{pp\to\tilde{q}\tilde{q}'(g)} + d\sigma^{\text{coll}}_{pp\to\tilde{q}\tilde{q}'(g)} + d\sigma^{\text{hard}}_{pp\to\tilde{q}\tilde{q}'g} + d\sigma^{\text{real-quark}}_{pp\to\tilde{q}\tilde{q}'\bar{q}^{(\prime)}}$$

Fully differential cross-section

NLO decay

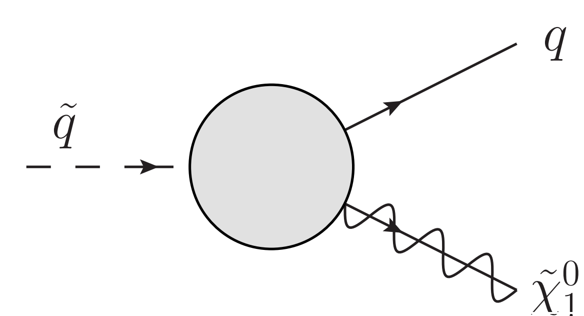

$$d\Gamma^{(1)}_{\tilde{q}\to q\tilde{\chi}^0_1} = d\Gamma^{\text{virtual+soft}}_{\tilde{q}\to q\tilde{\chi}^0_1(g)} + d\Gamma^{\text{coll}}_{\tilde{q}\to q\tilde{\chi}^0_1(g)} + d\Gamma^{\text{hard}}_{\tilde{q}\to q\tilde{\chi}^0_1 g}$$

Fully differential decay

NLO total decay width

$$\Gamma^{(0+1)}_{\tilde{q}\to q'\tilde{\chi}^\pm_j} = \Gamma^{(0)}\left[1 + \frac{4}{3}\frac{\alpha_s}{\pi}F^{QCD}\left(\frac{m_{\tilde{\chi}^\pm_j}}{m_{\tilde{q}}}, \frac{m_{\tilde{g}}}{m_{\tilde{q}}}\right)\right] \qquad \sum_{\chi^0_i,\chi^\pm_j}$$

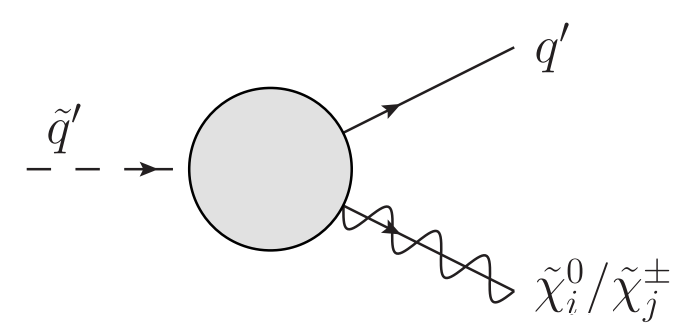

COMBINATION

For all different combinations of light flavours and chiralities, weighted events for squark-squark production are produced in the LAB frame.

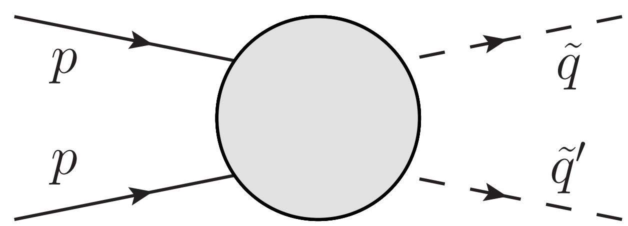

Weighted decay events are generated in the respective squark rest-frame.

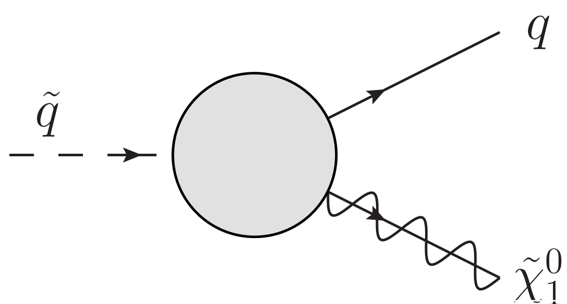

boost of decay events + "master formula"

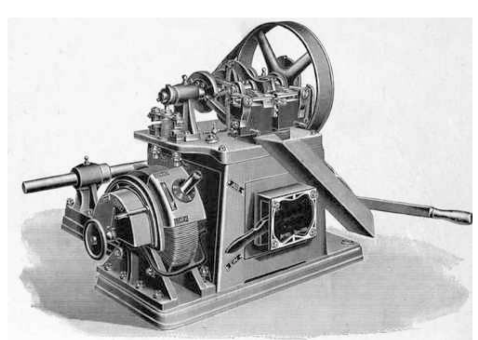

Fully differential distributions of factorizable NLO contributions in NWA.

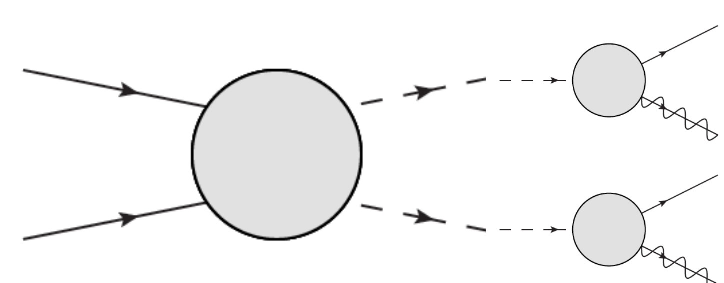

NUMERICAL RESULTS

We cluster partons into jets with anti-k_T algorithm, R=0.4 ATLAS and R=0.5 CMS and we always select jets according to:

$$p^{\mathrm{T}}_{j_{1/2}} > 20 \text{ GeV} \qquad |\eta_j| < 2.8,$$
$$p^{\mathrm{T}}_{j_i} > 50 \text{ GeV} \qquad |\eta_j| < 3.0 \text{ (for CMS observables)}$$

SPS1a (14 TeV)

Scale variation plots: $\mu_f = \mu_r = (m/2, m, 2m)$, m: average squark mass

SPS1a	$\tilde{u}_L$	$\tilde{u}_R$	$\tilde{d}_L$	$\tilde{d}_R$	$\tilde{g}$	$\tilde{\chi}^0_1$
mass (GeV)	563.6	546.7	569.0	546.6	608.5	97.0

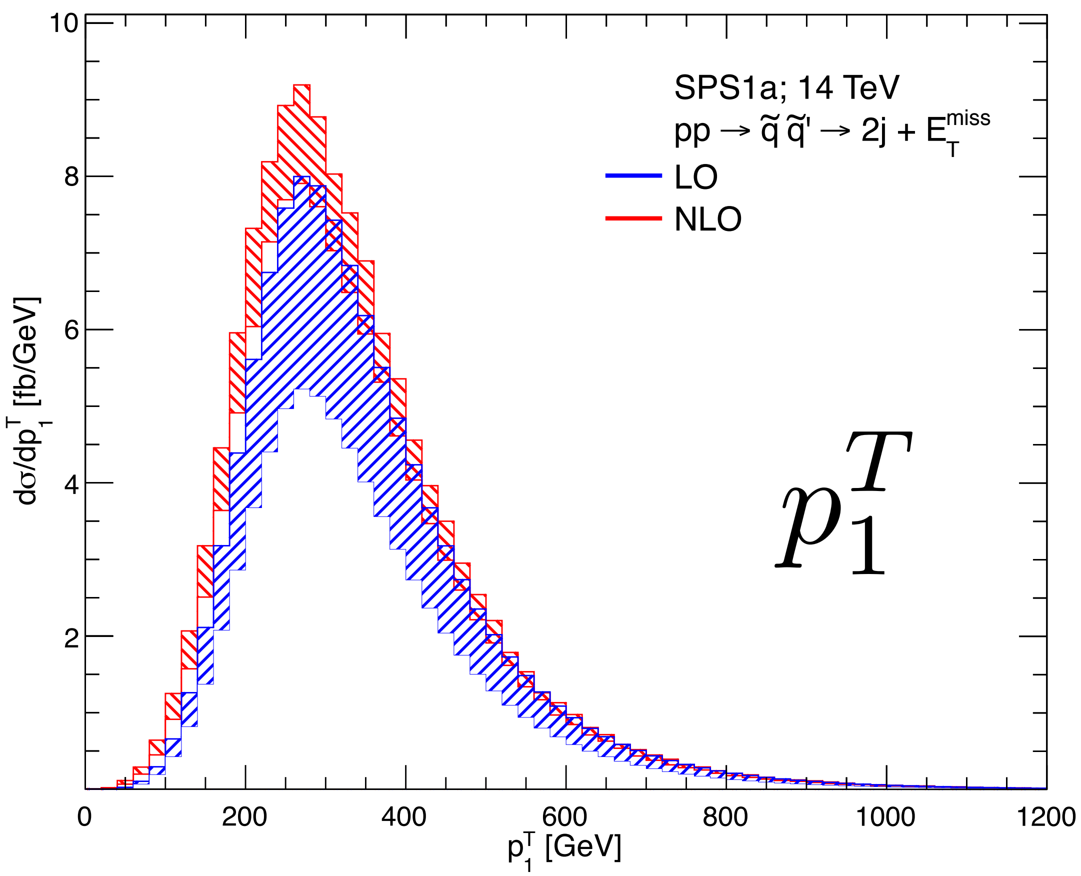

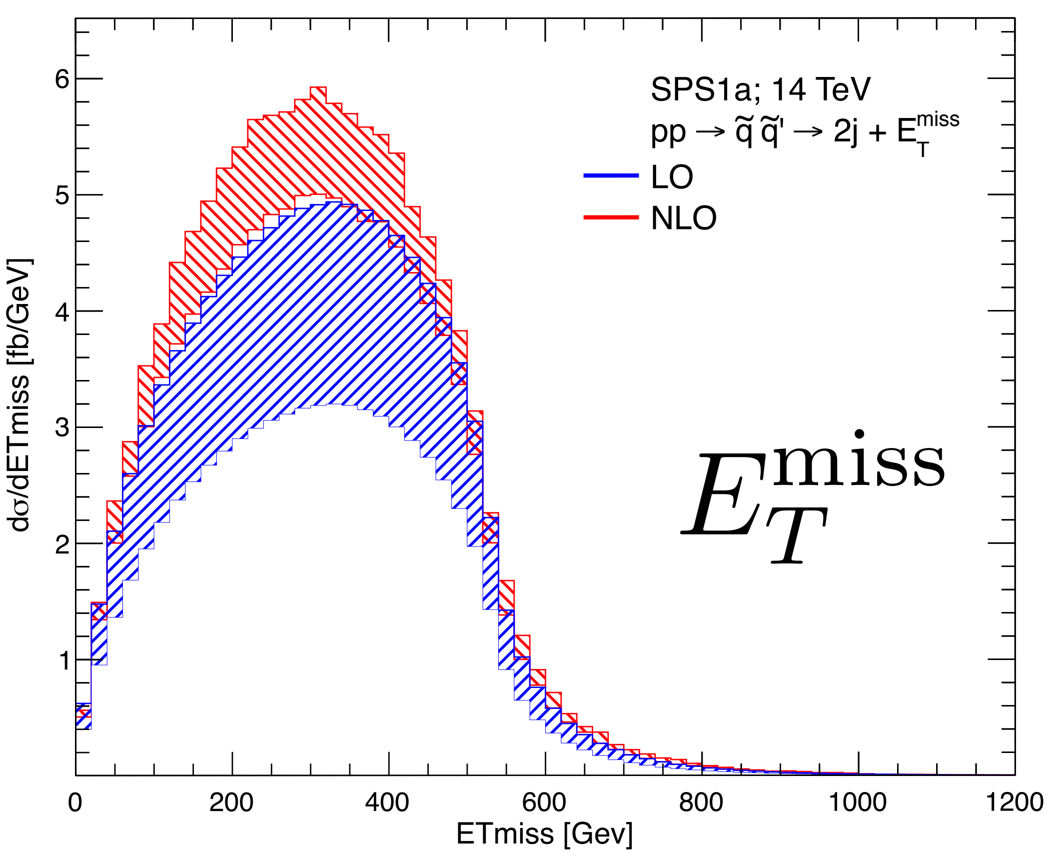

CMSSM 10.1.5 (14 TeV)

Comparison between NLO and LO rescaled by global K-factor: corrections purely in the shapes

10.1.5	$\tilde{u}_L$	$\tilde{u}_R$	$\tilde{d}_L$	$\tilde{d}_R$	$\tilde{g}$	$\tilde{\chi}_1^0$
mass (GeV)	1437.7	1382.3	1439.7	1376.9	1568.6	291.3

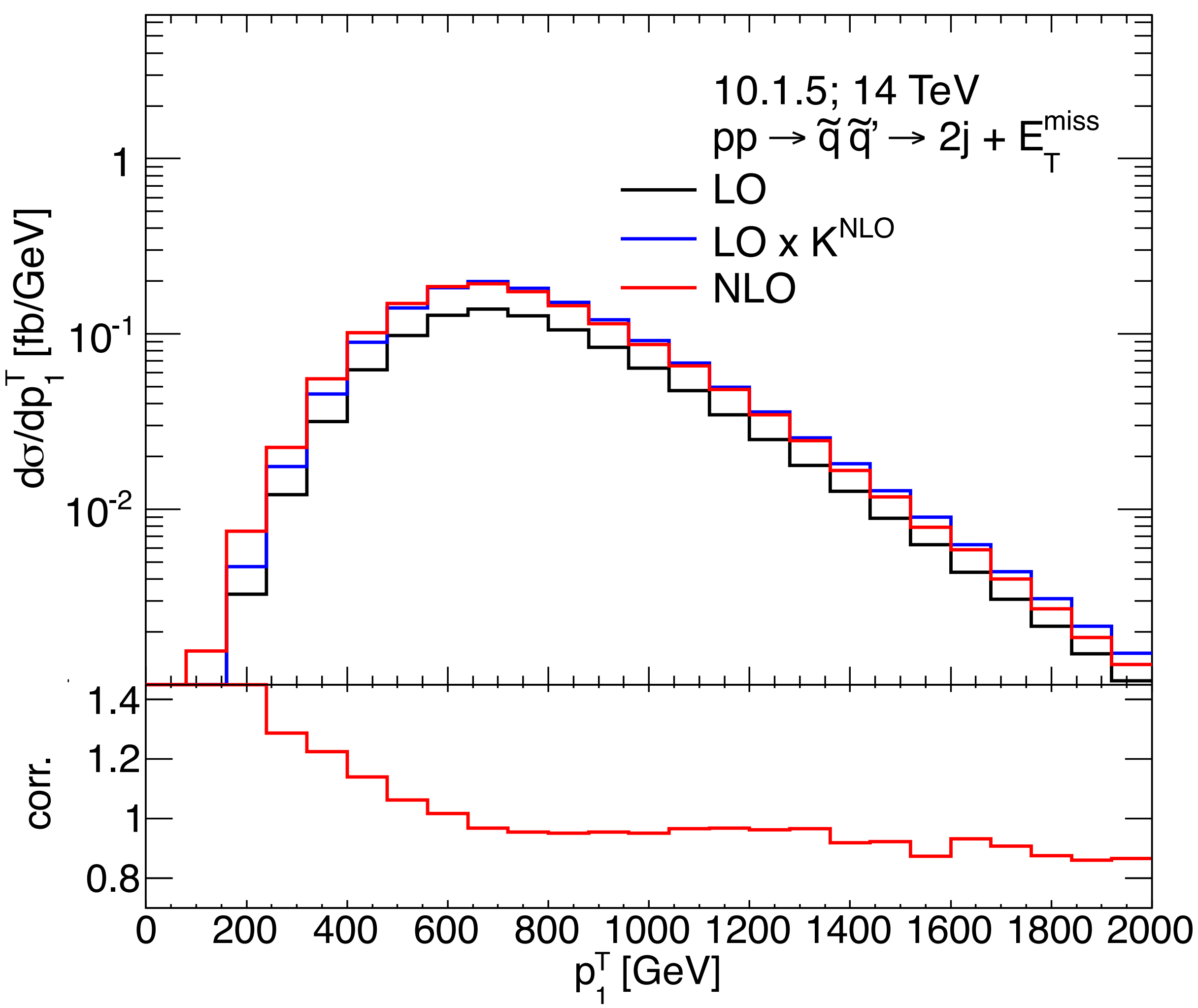

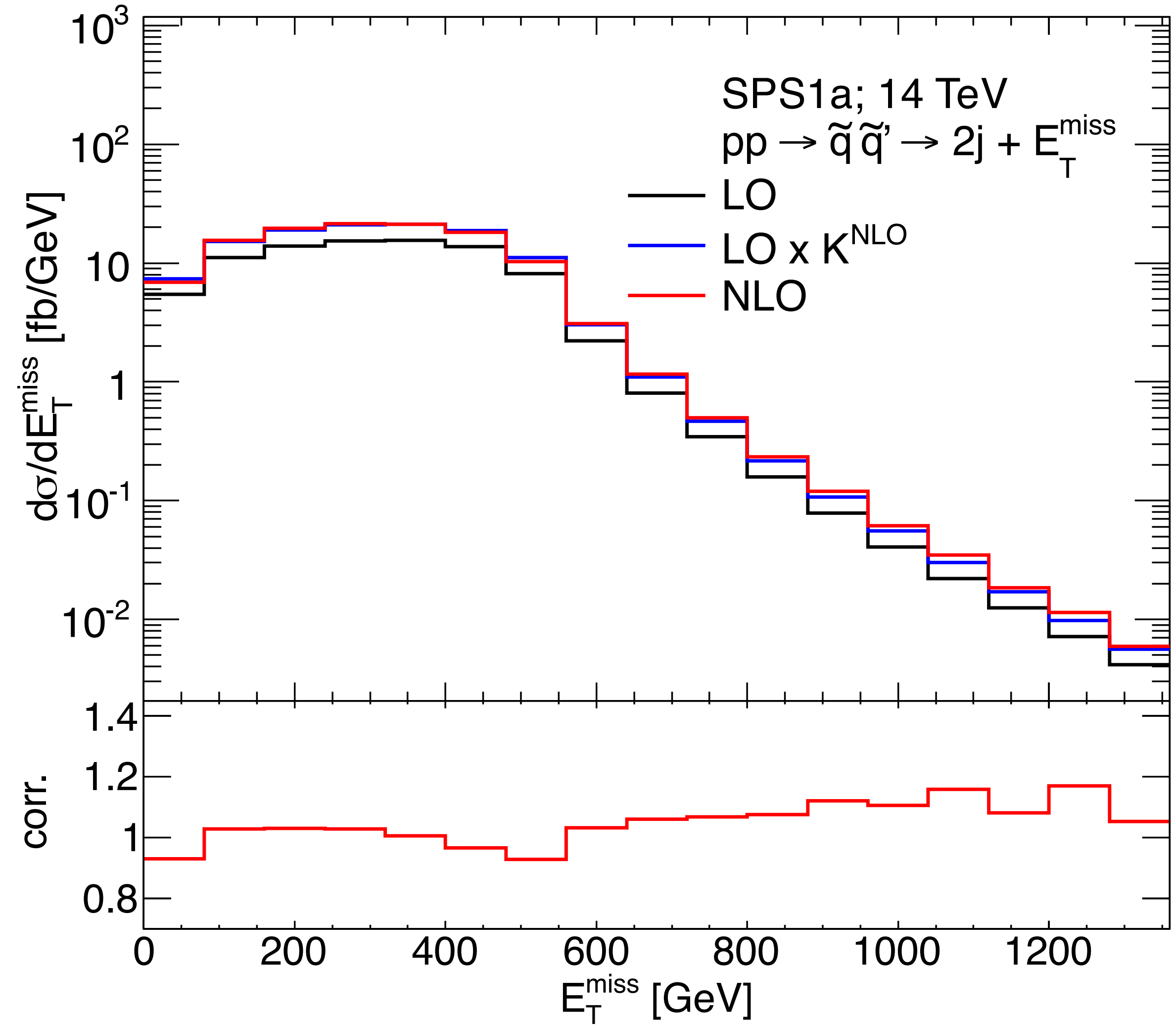

$$p_1^T$$

$$E_T^{\text{miss}}$$

CMSSM 10.1.5 (14 TeV)

Comparison between NLO and LO rescaled by global K-factor: corrections purely in the shapes

10.1.5	$\tilde{u}_L$	$\tilde{u}_R$	$\tilde{d}_L$	$\tilde{d}_R$	$\tilde{g}$	$\tilde{\chi}_1^0$
mass (GeV)	1437.7	1382.3	1439.7	1376.9	1568.6	291.3

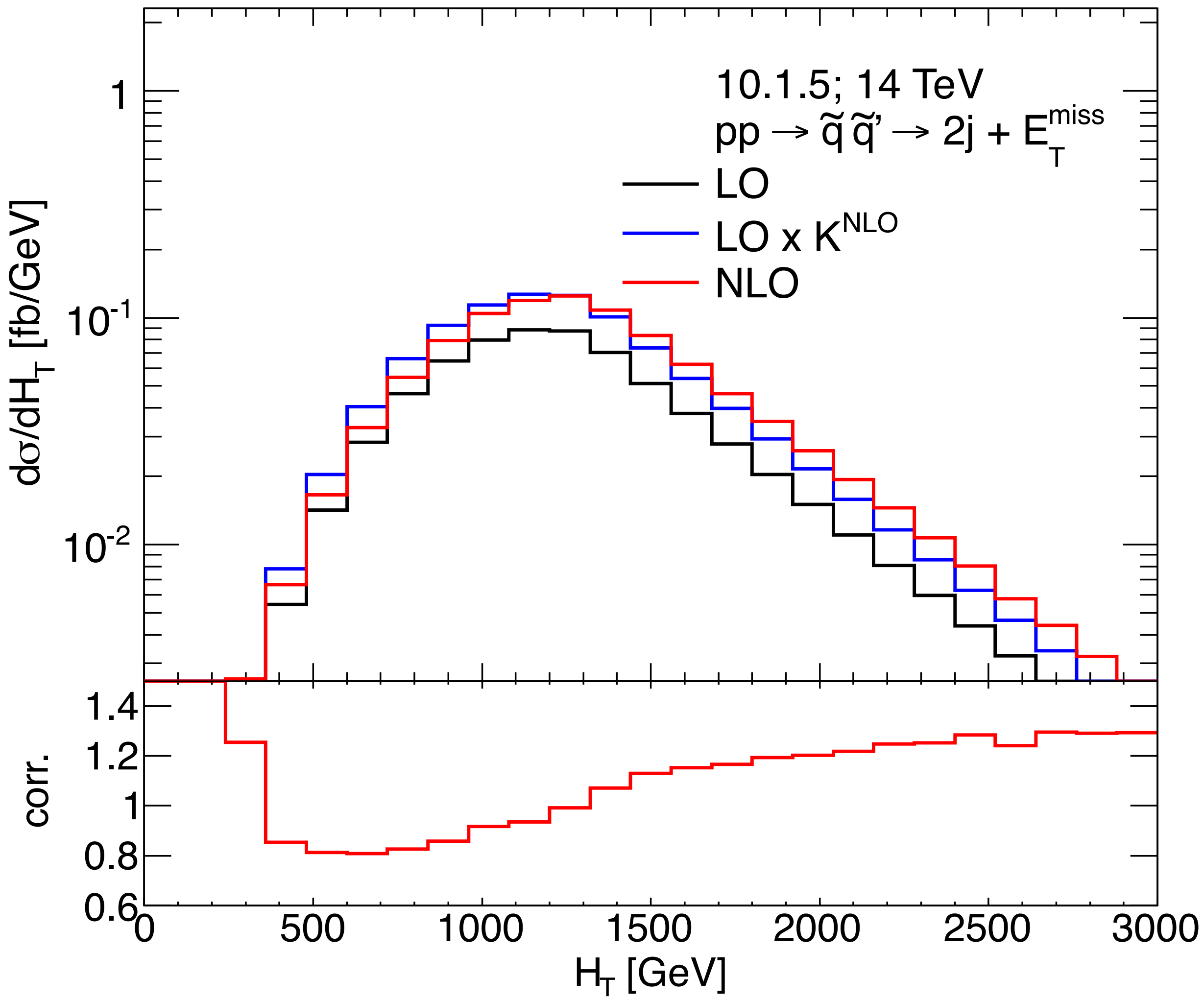

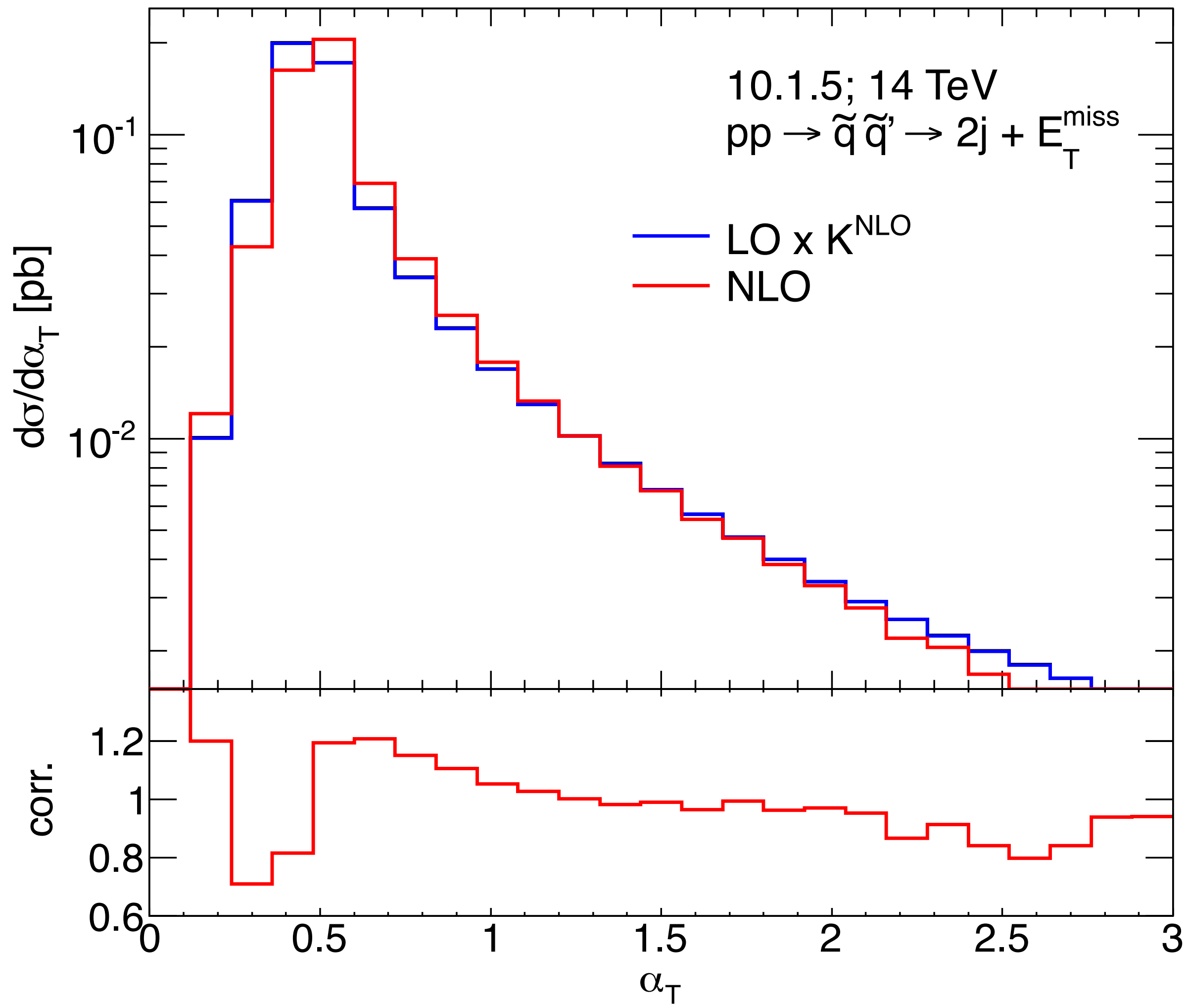

$$H_T = \sum_{i=1,2(,3)} p_i^{\mathrm{T}}$$

$$\alpha_T$$

p19MSSM1 (14 TeV)

Comparison between NLO and LO rescaled by global K-factor: corrections purely in the shapes

p19MSSM1	$\tilde{u}_L$	$\tilde{u}_R$	$\tilde{d}_L$	$\tilde{d}_R$	$\tilde{g}$	$\tilde{\chi}_1^0$
mass (GeV)	339.6	394.8	348.3	392.7	414.7	299.1

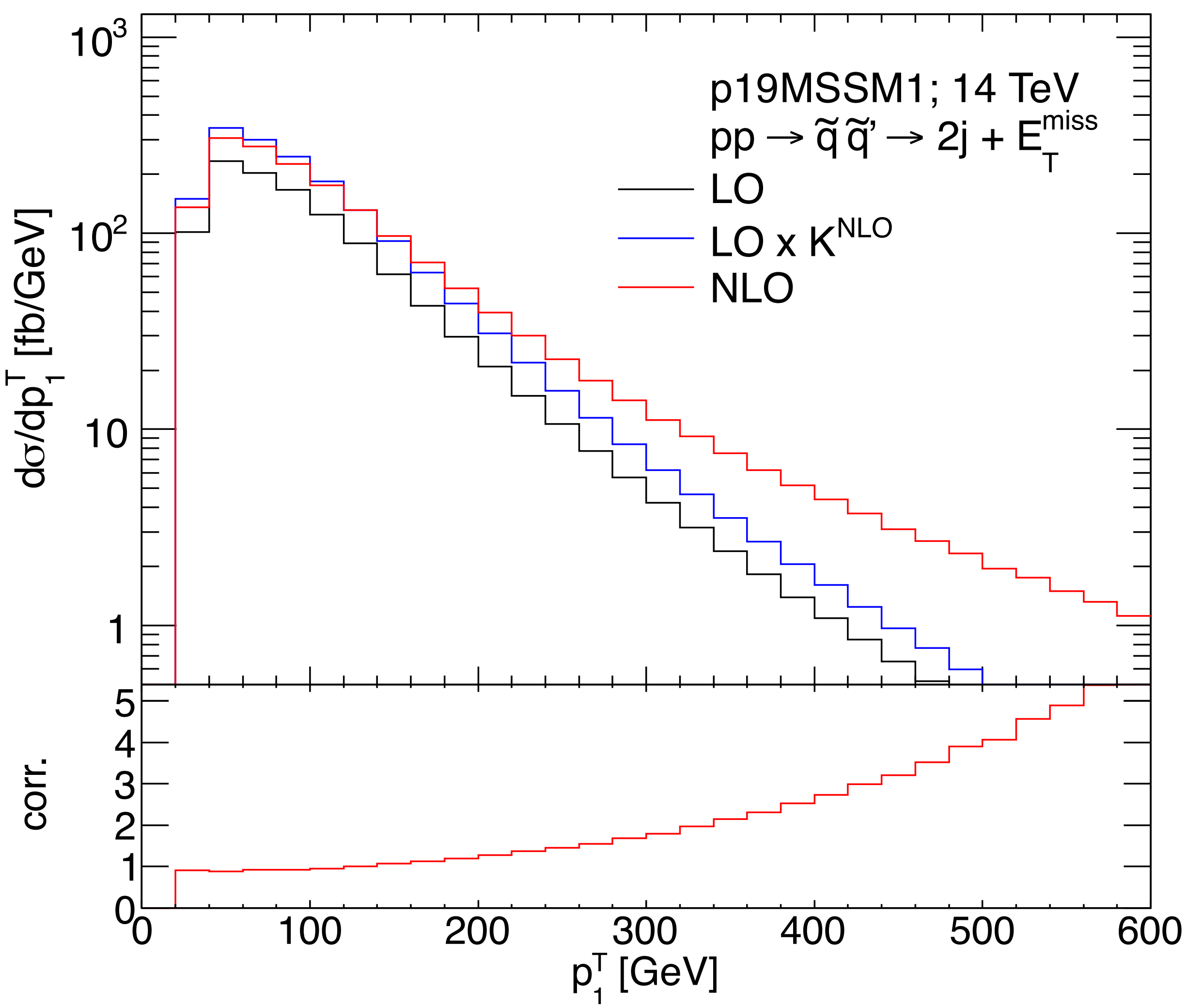

p_1^T

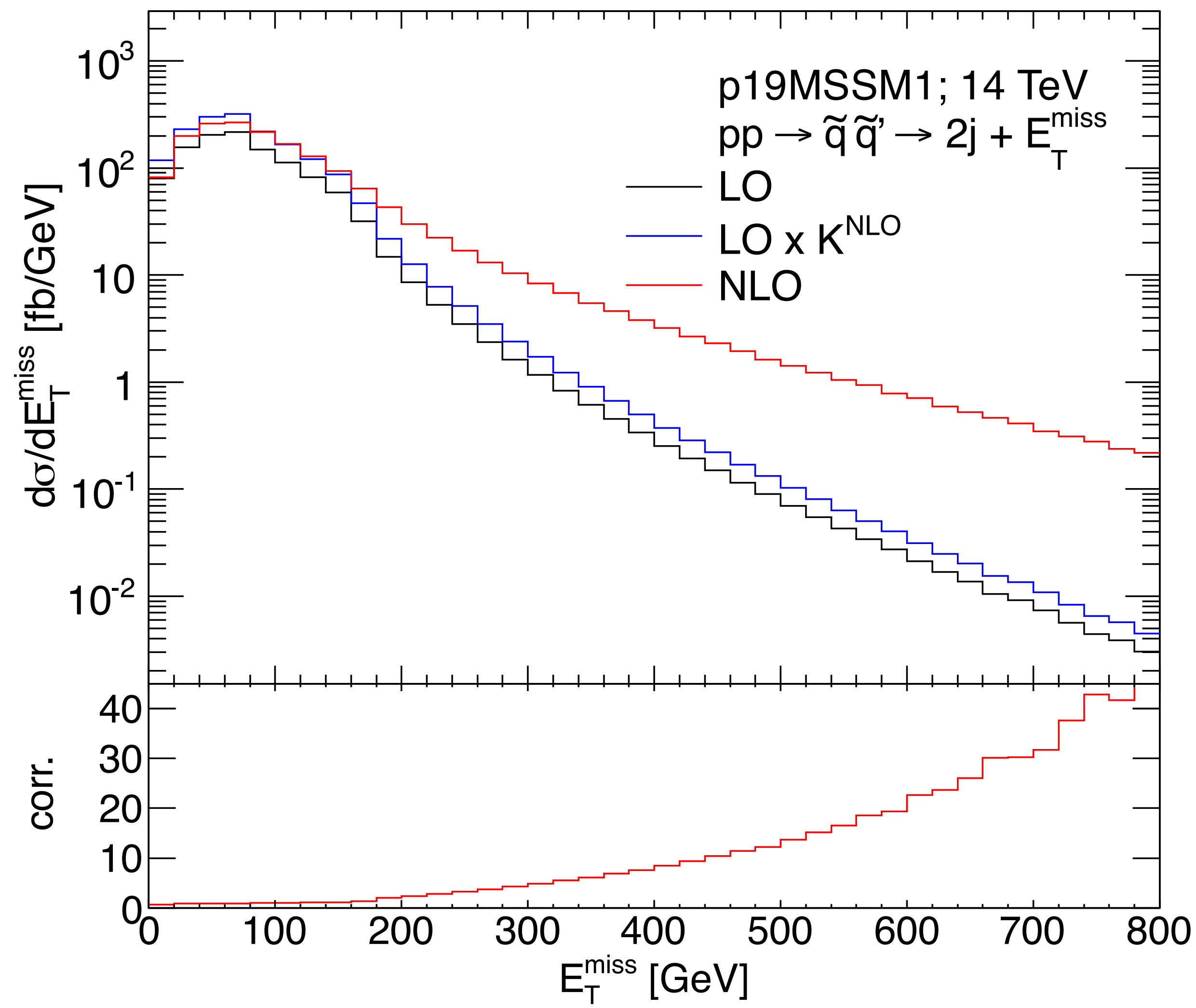

E_T^{miss}

Effect on cut-and-count searches performed by ATLAS.

Signal Region:

$$p^{\mathrm{T}}_{j_1} > 130\ \mathrm{GeV},\ p^{\mathrm{T}}_{j_2} > 40\ \mathrm{GeV},\ |\eta_{j_{1/2}}| < 2.8,\ \Delta\phi(j_{1/2}, \vec{\not{E}}_T) > 0.4$$
$$m_{\mathrm{eff}} > 1\ \mathrm{TeV},\ \not{E}_T/m_{\mathrm{eff}} > 0.3$$

benchmarkpoint	**Energy [TeV]**	$\boldsymbol{N^{(0)}_{\mathrm{ATLAS}}}$	$\boldsymbol{N^{(0+1)}_{\mathrm{ATLAS}}}$	$\boldsymbol{K_{N_{\mathrm{ATLAS}}}}$	$\boldsymbol{K_{pp\to\tilde{q}\tilde{q}'}}$
SPS1a	7	0.066 pb	0.083 pb	1.26	1.37
	8	0.097 pb	0.121 pb	1.25	1.35
	14	0.347 pb	0.424 pb	1.22	1.28
10.1.5	7	0.313 fb	0.503 fb	1.61	1.57
	8	0.861 fb	1.344 fb	1.56	1.52
	14	13.82 fb	19.77 fb	1.43	1.40
p19MSSM1	7	0.140 fb	20.76 fb	~ 150	1.40
	8	0.339 fb	37.96 fb	~ 110	1.39
	14	0.0044 pb	0.264 pb	~ 60	1.34

CONCLUSION

We provide a consistent fully differential calculation of factorizable NLO QCD corrections in NWA for squark-squark production and decay.

NLO corrections are, in general, important for precise description of physical observables.

In particular cases they can be essential for realistic description.

Fully differential NLO QCD prediction of production and decay for all squark/gluino channels are desirable.

Thank you for the attention.

Effect on cut-and-count searches performed by CMS.

benchmarkpoint	**Energy [TeV]**	$\boldsymbol{N^{(0)}_{\mathrm{CMS}}}$	$\boldsymbol{N^{(0+1)}_{\mathrm{CMS}}}$	$\boldsymbol{K_{N_{\mathrm{CMS}}}}$	$\boldsymbol{K_{pp\to\tilde{q}\tilde{q}'}}$
SPS1a	7	0.112 pb	0.141 pb	1.26	1.37
	8	0.157 pb	0.197 pb	1.25	1.35
	14	0.488 pb	0.614 pb	1.26	1.28
10.1.5	7	0.201 pb	0.261 pb	1.30	1.57
	8	0.542 fb	0.674 fb	1.24	1.52
	14	8.129 fb	8.884 fb	1.09	1.40
p19MSSM1	7	10^{-6} pb	0.095 pb	$\mathcal{O}(10^4)$	1.40
	8	10^{-6} pb	0.151 pb	$\mathcal{O}(10^4)$	1.39
	14	$2\cdot 10^{-5}$ pb	0.687 pb	$\mathcal{O}(10^4)$	1.34

Signal Region:

$$p^{\mathrm{T}}_{j_{1/2}} > 100 \text{ GeV},\ |\eta_{j_1}| < 2.5,\ |\eta_{j_2}| < 3.0,$$
$$H_T > 350 \text{ GeV},\ \not{H}_T/\not{E}_T < 1.25,\ \alpha_T > 0.55.$$

CMSSM 10.1.5 (14 TeV)
Contributions of the different flavour and chirality configurations

channel	$\sigma^{(0)}_{pp\to\tilde{q}\tilde{q}'}$ [fb]	$\sigma^{(0+1)}_{pp\to\tilde{q}\tilde{q}'}$ [fb]	$K_{pp\to\tilde{q}\tilde{q}'}$	$\sigma^{(0)}_{2j+\not{E}_T(+X)}$ [fb]	$\sigma^{(0+1)}_{2j+\not{E}_T(+X)}$ [fb]	$K_{2j+\not{E}_T(+X)}$
$\tilde{u}_L\tilde{u}_L$	7.08	9.44	1.33	$1.22\cdot10^{-3}$	$1.68\cdot10^{-3}$	1.38
$\tilde{u}_R\tilde{u}_R$	8.64	11.5	1.33	8.25	11.36	1.38
$\tilde{d}_L\tilde{d}_L$	1.07	1.44	1.36	$2.82\cdot10^{-4}$	$3.96\cdot10^{-4}$	1.40
$\tilde{d}_R\tilde{d}_R$	1.39	1.88	1.35	1.33	1.84	1.39
$\tilde{u}_L\tilde{u}_R$	6.00	8.49	1.42	$7.78\cdot10^{-2}$	$11.33\cdot10^{-2}$	1.45
$\tilde{d}_L\tilde{d}_R$	$8.20\cdot10^{-1}$	1.19	1.45	$1.32\cdot10^{-2}$	$1.96\cdot10^{-5}$	1.49
$\tilde{u}_L\tilde{d}_L$	8.25	11.9	1.44	$1.76\cdot10^{-3}$	$2.62\cdot10^{-3}$	1.49
$\tilde{u}_R\tilde{d}_R$	10.5	15.1	1.44	10.00	14.92	1.49
$\tilde{u}_L\tilde{c}_L$	$3.28\cdot10^{-1}$	$4.33\cdot10^{-1}$	1.32	$5.65\cdot10^{-5}$	$7.73\cdot10^{-5}$	1.37
$\tilde{u}_R\tilde{c}_R$	$4.29\cdot10^{-1}$	$5.74\cdot10^{-1}$	1.34	$4.09\cdot10^{-1}$	$5.68\cdot10^{-1}$	1.39
$\tilde{d}_L\tilde{s}_L$	$1.95\cdot10^{-1}$	$2.75\cdot10^{-1}$	1.41	$5.16\cdot10^{-5}$	$7.5097\cdot10^{-5}$	1.46
$\tilde{d}_R\tilde{s}_R$	$2.71\cdot10^{-1}$	$3.87\cdot10^{-1}$	1.42	$2.59\cdot10^{-1}$	3.82	1.48
$\tilde{u}_L\tilde{d}_R$	2.44	3.50	1.44	$3.16\cdot10^{-2}$	$4.67\cdot10^{-2}$	1.48
$\tilde{u}_R\tilde{d}_L$	2.40	3.46	1.44	$3.87\cdot10^{-2}$	$5.70\cdot10^{-2}$	1.48
$\tilde{u}_L\tilde{c}_R$	$1.69\cdot10^{-1}$	$2.39\cdot10^{-1}$	1.41	$2.19\cdot10^{-3}$	$3.18\cdot10^{-3}$	1.46
$\tilde{d}_L\tilde{s}_R$	$9.51\cdot10^{-2}$	$1.39\cdot10^{-1}$	1.46	$1.52\cdot10^{-3}$	$2.29\cdot10^{-3}$	1.50
sum	50.04	69.86	1.40	20.41	29.32	1.44

p19MSSM1 (14 TeV)
Comparison between NLO and LO rescaled by global K-factor: corrections purely in the shapes

p19MSSM1	$\tilde{u}_L$	$\tilde{u}_R$	$\tilde{d}_L$	$\tilde{d}_R$	$\tilde{g}$	$\tilde{\chi}_1^0$
mass (GeV)	339.6	394.8	348.3	392.7	414.7	299.1

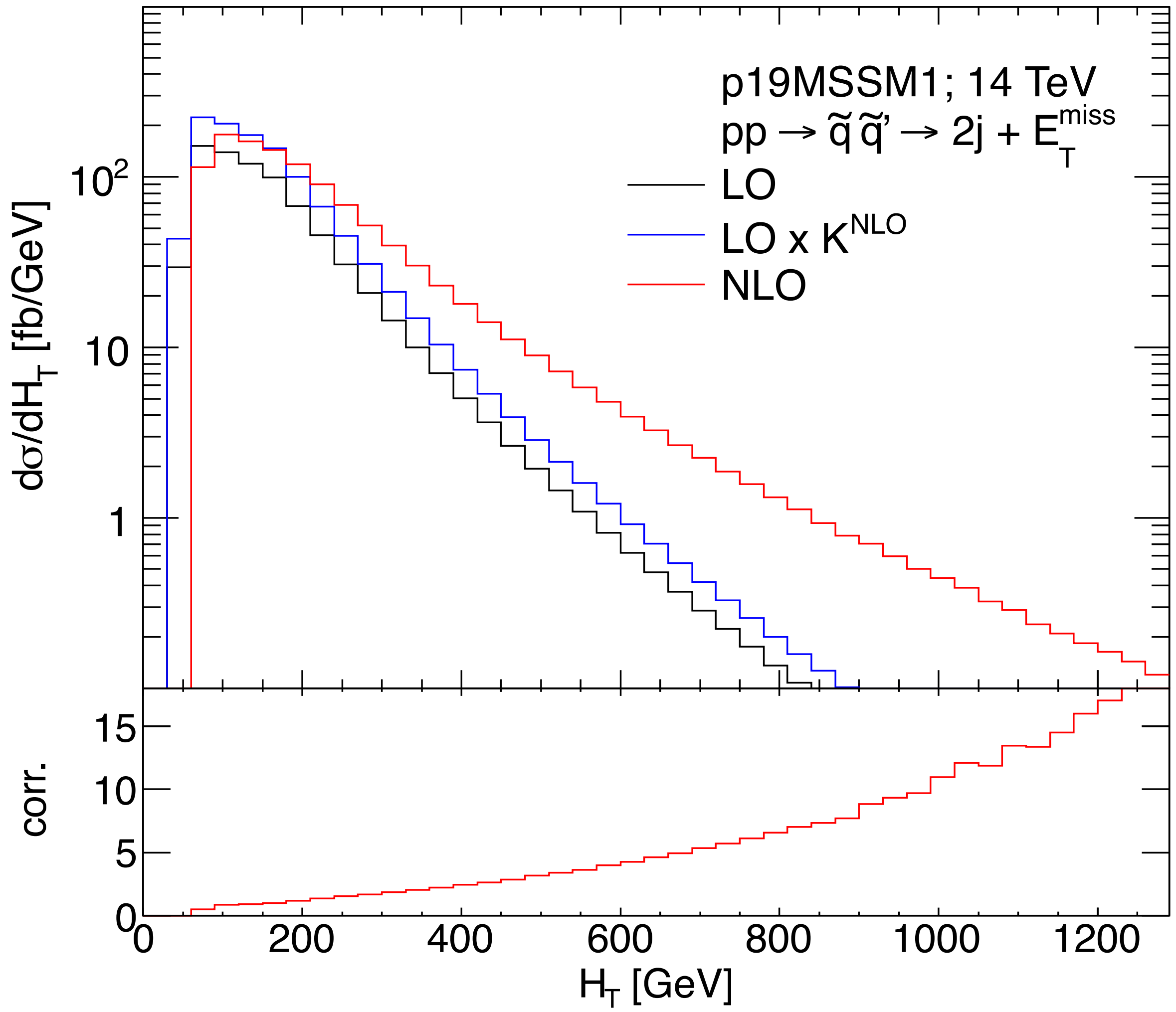

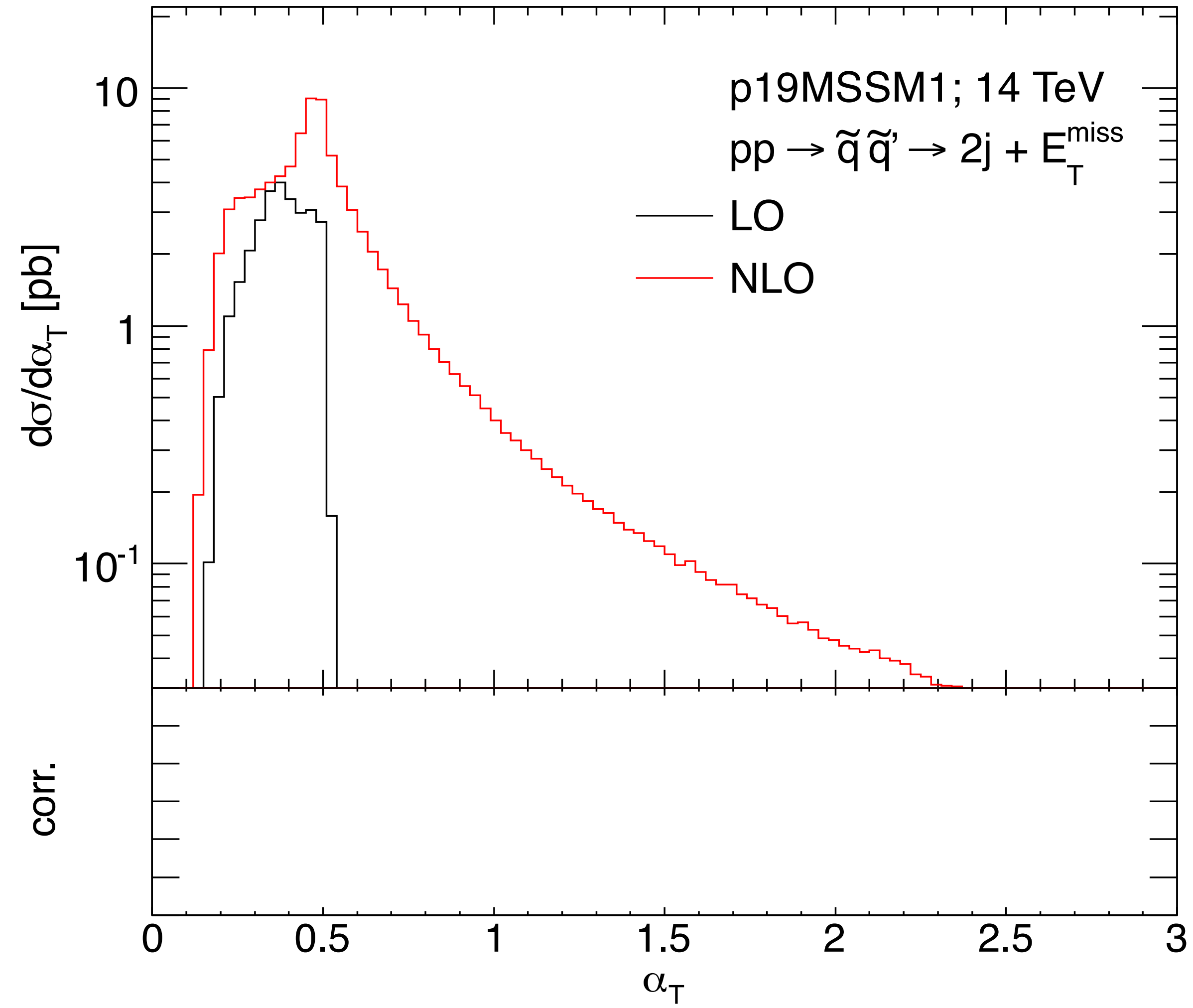

$$H_T = \sum_{i=1,2(,3)} p_i^{\mathrm{T}} \qquad\qquad \alpha_T$$